

Internal multiple attenuation for OBN data with overburden/target separation

Roberto Pereira*, Mena Ramzy, Petre Griscenco, Benjamin Huard, Hui Huang, Luis Cypriano, and Adel Khalil
(CGG)

Summary

Ocean bottom node (OBN) acquisitions provide the increased illumination necessary for imaging deep targets below complex overburdens. In such cases, internal multiples can also be detrimental to the image at the target level. Following the concept of “overburden/target separation” for internal multiple attenuation (IMA) introduced by van der Neut and Wapenaar (2016), we extend the formulation to be applicable to ocean bottom recordings. We demonstrate the results for up-going and down-going wavefields on a data set from the Santos Basin, offshore Brazil, where internal multiple contamination is a widely recognized imaging problem.

Introduction

Areas with complex overburdens pose a major challenge for seismic imaging of deep targets. Reduced illumination can compromise velocity estimation and the image at the target level. A solution to this problem is given by ocean bottom node acquisitions. These provide increased illumination through larger offsets and full azimuthal coverage (Bunting and Moses, 2016). In these complex areas, another issue that might arise is that of internal multiples. Strong reflectors in the overburden can generate internal multiples, which will be imaged incorrectly as artifacts. These artifacts may have detrimental effects on interpretation and amplitude analysis.

The pre-salt area in the Santos Basin, offshore Brazil is a good example of this scenario, where both illumination and internal multiples affect the imaging in the target areas. One of the characteristics of this basin is the presence of stratified salt. This makes it particularly challenging for internal multiple prediction, since the identification of the generators inside the salt is impractical.

The problem of internal multiples in the Santos Basin has received some attention in the last few years in the case of streamer acquisitions (Hembd et al., 2011; Cypriano et al., 2015). An IMA method based on the Marchenko equations has recently been proposed and tested on a few streamer acquisitions from the Santos Basin (van der Neut and Wapenaar, 2016; Pereira et al., 2018; Krueger et al., 2018). It relies on the separation of the data in overburden/target regions, rather than the identification of internal multiple generators (Jakubowicz, 1998).

A full solution tailored to OBN acquisitions is still lacking. In this abstract, we extend the streamer method of van der

Neut and Wapenaar (2016) to the OBN case. We then apply this approach to an OBN data set from the Santos Basin, for both up- and down-going wavefields.

Method

In Pereira et al. (2018), one of the models proposed in van der Neut and Wapenaar (2016) is described. This streamer implementation is shot-based and has two main steps. First a crosscorrelation operator is applied to the data, constructing a so-called ‘virtual shot’ (Ikelle, 2006). Then, a convolution operator is applied. To avoid primary leakage, some mutes are designed. In particular, a mute is applied in the virtual shot domain, which has the effect of separating primary from multiple energy without prior knowledge of generators.

Moving on to the OBN case, we use reciprocity and make the implementation receiver based. Since this is the most populated gather in the acquisition, this will save on computation. The model is given by the following expression:

$$M_h(x_s, x_r; t) = -\{\Theta_{t_h}^{\infty} \mathbf{R} \Theta_{t_0}^{t_h} \mathbf{R}^* \Theta_{t_0}^{t_h} \mathbf{R}\} (x_s, x_r; t). \quad (1)$$

It is defined for a given horizon h separating the data into overburden and target regions. $R(x, x_r; t)$ is the node data at receiver position x_r . \mathbf{R} and \mathbf{R}^* represent the convolution and crosscorrelation operators, respectively. They are constructed out of reflection data defined at the sea datum. Θ_a^b is a mute function defined to be equal to one between a and b , and zero elsewhere. t_h is the two-way traveltime corresponding to horizon h , consistent with the wavefield configuration i.e. up- or down-going. t_0 is the mute time applied in the virtual domain mentioned above.

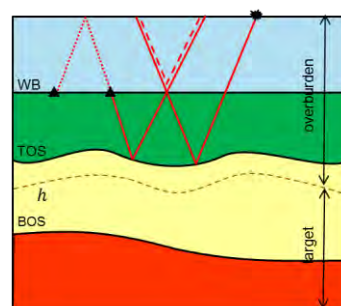


Figure 1: Cartoon representing an internal multiple event. The dotted red line represents the extra travel time of the down-going wavefield. An example of overburden/target separation is given by the dashed brown line.

Internal multiple attenuation for OBN data

Figure 1 represents an internal multiple event modeled by this equation, for both up- and down-going components. The dashed red line represents a trace coming from \mathbf{R}^* . It can be thought of as having negative time, effectively creating a downward reflector at the subsurface.

The main difference between the streamer and the OBN implementations is in the definition of the mute functions. The key mute time given by t_0 , is applied in the virtual gather domain. The cartoon in Figure 2d represents one particular event in this gather. Its traveltime corresponds to the direct wave between the receiver position and the sea surface. It is negative for the up-going and positive for the down-going. Convolving this virtual event with the surface trace at the source side would again construct a primary event. To avoid this occurrence, a mute t_0 can be designed as follows:

$$t_0 = \pm \sqrt{z^2 + x^2} / c_0 + \epsilon . \quad (2)$$

z is the receiver depth, x the offset in this virtual gather, c_0 is the water velocity and ϵ a small number. The sign is positive for down-going and negative for up-going. The limit of z going to zero corresponds to the streamer case. Examples of t_0 for the streamer and OBN down- and up-going are shown in Figures 2(a-c) by the blue lines.

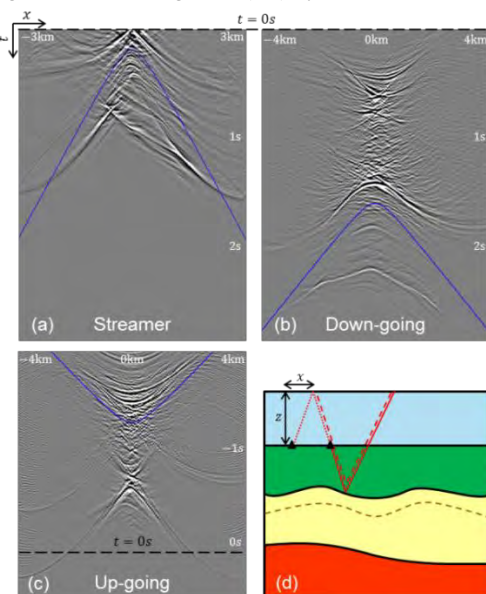


Figure 2: Mute in the virtual domain for (a) streamer, (b) OBN down-going, and (c) OBN up-going cases. (d) shows a virtual event that will generate primary leakage in the model if not muted.

The data necessary to construct operators \mathbf{R} and \mathbf{R}^* is not readily available in the case of ocean bottom recordings. In the context of SRME (Verschuur et al., 1992) for OBN data sets, two possible solutions for this have been proposed.

The first is to combine OBN data with auxiliary surface streamer data sets covering the same area (Verschuur and Neumann, 1999). Such data sets are usually available in deep water areas, since OBN surveys come at a later stage of the exploration cycle. The second alternative is to use modeling based on a reflectivity model (Pica et al., 2006). In the following example, we use an auxiliary streamer data set.

OBN field data example

We applied the method described above to an OBN data set from the Santos Basin that shows strong contamination from internal multiples. The water depth for this survey is around 2100 m. A towed streamer data set covering the same area was used to construct operators \mathbf{R} and \mathbf{R}^* .

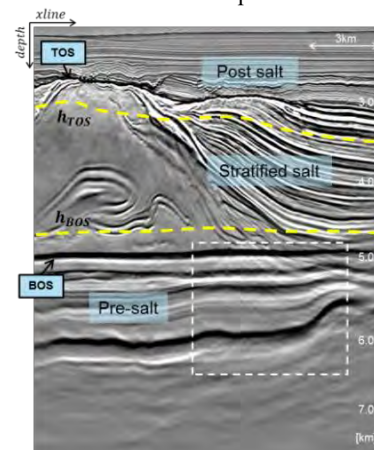


Figure 3: OBN down-going stack section from the Santos Basin. The two horizons used to construct the internal multiple models are shown by the dashed yellow lines. The dashed white box indicates the zoomed-in area of Figure 6.

In order to minimize spectral differences with the OBN data, the streamer data set received a full broadband pre-processing flow, including signature, source/receiver deghosting, and SRME. It was further interpolated in order to de-alias operators \mathbf{R} and \mathbf{R}^* . The OBN data set received its own broadband pre-processing flow, including PZ sum to separate up- and down-going components, signature, source deghosting, and SRME.

Figure 3 shows a Kirchhoff pre-stack depth migration stacked section from the OBN data set. It has a thick layer of salt with stratification on the right. The salt layer separates the post-salt from the pre-salt region, which is where most targets are located in this basin. Looking at the pre-salt area, cross-cutting events can be observed, especially in the dashed white box. These correspond to internal multiples generated by reflectors located in the post-salt and in the stratified salt.

Internal multiple attenuation for OBN data

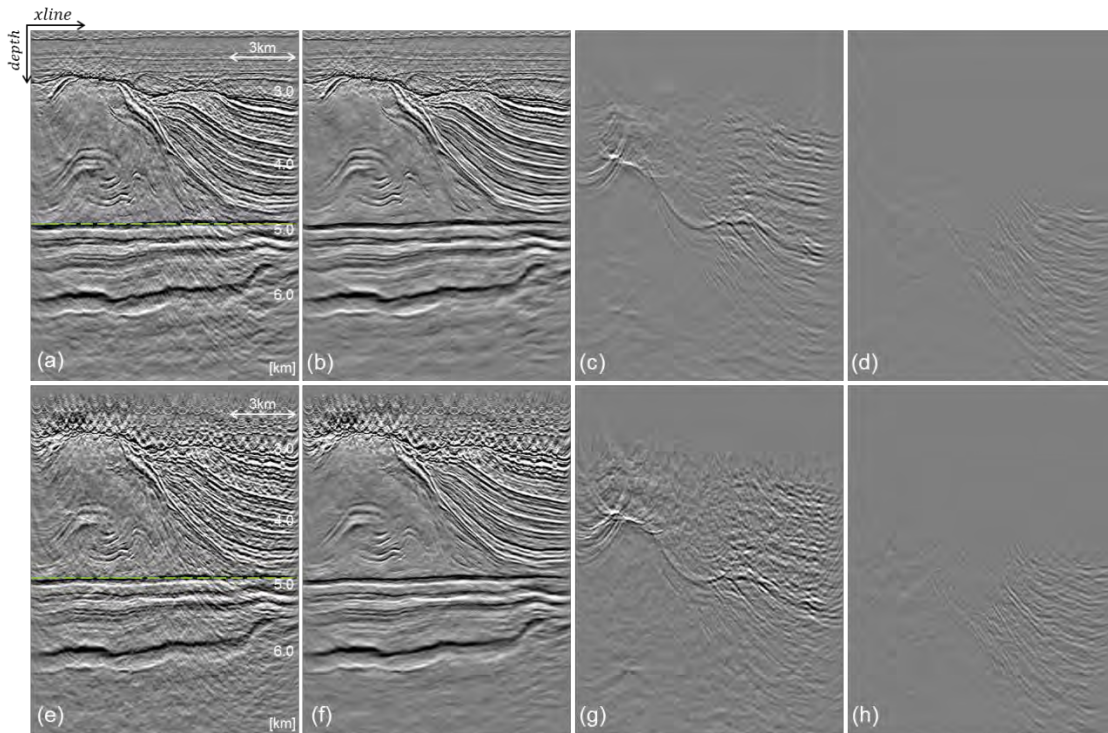


Figure 4: Inline section from a near offset COV. Top: (a) input, (b) subtraction output, (c) TOS model, and (d) (BOS-TOS) model for the down-going wavefield. Bottom: (e) input, (f) subtraction output, (g) TOS model, and (h) (BOS-TOS) model for up-going wavefield. Depth slice in Figure 5 is indicated by the dashed green line.

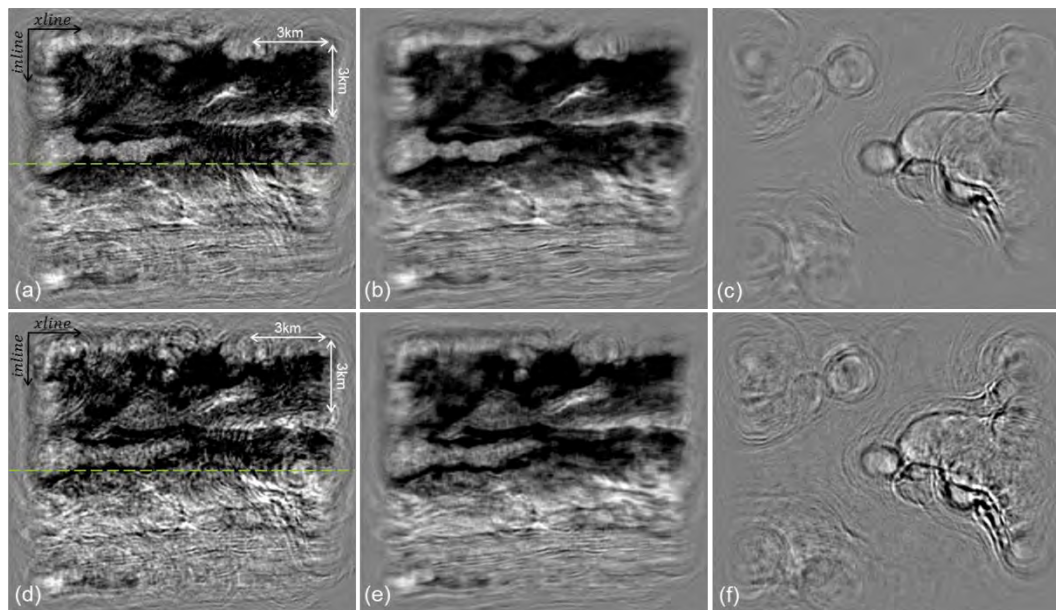


Figure 5: Depth slice of 4900 m from a near offset COV. Top: (a) input, (b) subtraction output, and (c) TOS model for the down-going wavefield. Bottom: (d) input, (e) subtraction output, and (f) TOS model for the up-going wavefield. Inline in Figure 4 is indicated by dashed green line.

Internal multiple attenuation for OBN data

Considering the complexity of the internal multiples present in this data set, we produced two different models based on different definitions of the overburden/target regions. The first used a horizon placed just below the top of salt (TOS), while the second used a horizon placed just above the base of salt (BOS). We will refer to them loosely as the TOS and BOS models, respectively.

One of the characteristics of the model in Equation 1 is that the deeper the horizon h , the more multiples are included, as long as they arrive after t_h . With that in mind, we can take the difference between the TOS and BOS models, and mute it at the later time to define a new model, that we refer to as the (BOS-TOS) model. We will see that the multiples present in the TOS and (BOS-TOS) models have different characteristics in terms of amplitude and move-out. The point of this manipulation is to make the subtraction as orthogonal as possible.

We computed the model in Equation 1 for each node and for both of the horizons defined above. We then separated the input and each internal multiple model into common offset vectors (COVs) and migrated each COV from each data set independently. Adaptive subtraction was performed on the migrated COVs with the help of 3D curvelet filters (Wu and Hung, 2015). Both TOS and (BOS-TOS) models were adapted simultaneously to the input.

Figure 4 shows the subtraction results and models for a near offset COV, for both down-going and up-going components. We observe that the input sections are greatly contaminated by internal multiple artifacts and that after subtraction we obtain a much cleaner section. The TOS model contains the dominant internal multiples, generated by the top of salt itself together with post-salt reflectors, while the (BOS-TOS) model isolates internal multiples generated by the stratified salt. We also observe a consistency between up- and down-going multiples, which is expected for a near-offset COV.

Figure 5 shows depth slices for the same near-offset COV, again for both up- and down-going components. The depth slice was taken at 4900 m depth. This time we show only the TOS model. It shows a clear imprint of the overburden on the image of the target area that is recognizable in the input. After subtraction, we observe a more coherent image with features consistent with the geology at that depth.

Figures 6(a-c) show results for a zoomed part of the same stack shown in Figure 3. This time we show only the (BOS-TOS) model. Multiples that survive the stack (an example is indicated by the green arrow in Figure 6a) correlate with multiples in the (BOS-TOS) model (Figure 6c). This

observation is confirmed by the gathers shown in Figures 6(d-f), where the model in Figure 6f shows flat events.

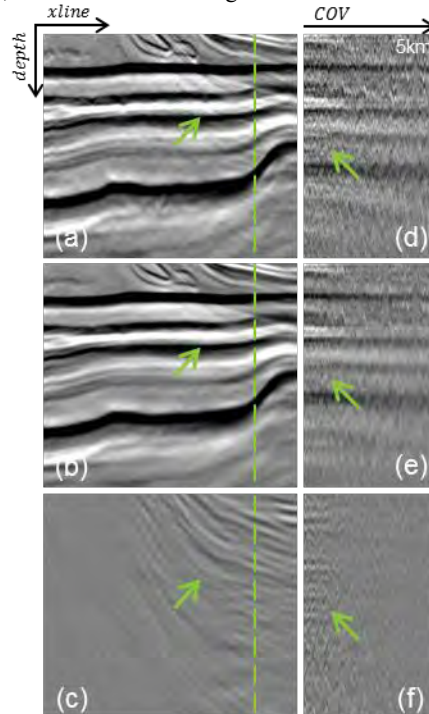


Figure 6: Zoomed area of stack from down-going wavefield and corresponding CDP-COV gathers with offsets up to 5km. Left: (a) input, (b) subtraction output, and (c) (BOS-TOS) model. Right: (d) input, (e) subtraction output and (f) model. Gather location is indicated by the green dashed line. Internal multiples are indicated by the green arrows.

Conclusions

We generalized the internal multiple attenuation method of van der Neut and Wapenaar (2016) to ocean bottom acquisitions. We described our prediction and subtraction strategies and applied IMA with overburden/target separation to an OBN data set from the Santos Basin. The results showed a clear improvement with attenuated artifacts from internal multiples in the final image. The proposed method does not rely on the identification of internal multiple generators, making it particularly useful in the context of the Santos Basin.

Acknowledgments

We would like to thank Petrobras for discussions and technical contributions as well as permission to publish the images. We thank CGG for permission to publish this abstract.

REFERENCES

- Bunting, T., and J., Moses, 2016, The transformation of seabed seismic: First Break, **34**, 119–164.
- Cypriano, L., F., Marpeau, R., Brasil, G., Welter, H., Prigent, H., Douma, M., Velasques, J., Boechat, P., de Carvalho, C., Guerra, and C., Theodoro, 2015, The impact of inter-bed multiple attenuation on the imaging of pre-salt targets in the Santos basin off-shore Brazil: 77th Annual International Conference and Exhibition, EAGE, Extended Abstracts, Tu N114 06.
- Hembd, J., M., Griffiths, C., Ting, and N., Chazalnoel, 2011, Application of 3D interbed multiple attenuation in the Santos Basin, Brazil: 73rd Annual International Conference and Exhibition, EAGE, Extended Abstracts, H047.
- Ikelle, L. T., 2006, A construct of internal multiples from surface data only: The concept of virtual seismic events: Geophysical Journal International, **164**, 383–393.
- Jakubowicz, H., 1998, Wave equation prediction and removal of interbed multiples: 68th Annual International Meeting, SEG, Expanded Abstracts, 1527–1530, doi: <https://doi.org/10.1190/1.1820204>.
- Krueger, J., D., Donno, R., Pereira, D., Mondini, A., Souza, J., Espinoza, and A., Khalil, 2018, Internal multiple attenuation for four presalt fields in the Santos Basin, Brazil: 88th Annual International Meeting, SEG, Expanded Abstracts, 4523–4527, doi: <https://doi.org/10.1190/segam2018-2990024.1>.
- Pereira, R., D., Mondini, and D., Donno, 2018, Efficient 3D internal multiple attenuation in the Santos basin: 80th Annual International Conference and Exhibition, EAGE, Extended Abstracts, We C 08.
- Pica, A., M., Manin, P. Y., Granger, D., Marin, E., Suaudeau, B., David, G., Poulaing, and P. H., Herrmann, 2006, 3D SRME on OBS data using waveform multiple modeling: 76th Annual International Meeting, SEG, Expanded Abstracts, 2659–2663, doi: <https://doi.org/10.1190/1.2370074>.
- van der Neut, J., and K., Wapenaar, 2016, Adaptive overburden elimination with the multidimensional Marchenko equation: Geophysics, **81**, no. 5, T265–T284, doi: <https://doi.org/10.1190/geo2016-0024.1>.
- Verschuur, D. J., A. J., Berkhouit, and C. P. A., Wapenaar, 1992, Adaptive surface-related multiple elimination: Geophysics, **57**, 1166–1177, doi: <https://doi.org/10.1190/1.1443330>.
- Verschuur, D. J., and E. I., Neumann, 1999, Integration of OBS data and surface data for OBS multiple removal: 69th Annual International Meeting, SEG, Expanded Abstracts, 1350–1353, doi: <https://doi.org/10.1190/1.1820762>.
- Wu, X., and B., Hung, 2015, High-fidelity adaptive curvelet domain primary-multiple separation: First Break, **33**, 13–59.